

Very low amplified spontaneous emission threshold from a molecular host-guest energy-transfer system and electroluminescence from light-emitting diode structure

Stefano Toffanin*, Raffaella Capelli, Gianluca Generali, Tsy-Yuan Hwu⁺, Ken-Tsung Wong⁺, Roberto Zamboni, Michele Muccini

Consiglio Nazionale delle Ricerche (CNR), Istituto per lo Studio dei Materiali Nanostrutturati (ISMN), via P. Gobetti 101, I-40129 Bologna, Italy

⁺Department of Chemistry, National Taiwan University, Taipei 106, Taiwan

Abstract

We report on the characteristics of a host-guest lasing system obtained by co-evaporation of an oligo(9,9-diaryluorene) derivative named T3 with the red-emitter 4-(dicyanomethylene)-2-methyl-6-(p-dimethylaminostyryl)-4H-pyran dye (DCM). We demonstrate that the ambipolar semiconductor T3 can be implemented as active matrix in the realization of a host-guest system in which an efficient energy transfer takes place from T3 matrix to the lasing DCM molecules. We performed a spectroscopic study on the system by systematically varying the DCM concentration in the T3 matrix. Measurements of steady-state photoluminescence (PL), PL quantum yield (PLQY) and amplified spontaneous emission (ASE) threshold are used to optimize the acceptor concentration at which the ASE from DCM molecules takes place with the lowest threshold.

Organic light-emitting diodes (OLEDs) implementing the DCM:T3 host-guest system as recombination layer are fabricated for verifying the optical properties of the optimised blend in real working devices.

Indeed, the very low ASE threshold of T3:DCM makes the investigated blend an appealing system for use as active layer in lasing devices. In particular, the ambipolar charge transport properties of the T3 matrix and its field-effect characteristics make the host-guest system presented here an ideal candidate for the realization of electrically-pumped organic lasers.

Keywords: ASE threshold, host-guest system, diaryluorene derivative, energy transfer, OLED

1. INTRODUCTION

Organic light emitting materials are attractive gain media for use in semiconductor lasers. Optically pumped laser action has been demonstrated in a broad range of materials in many different configurations with emission wavelengths covering the entire visible spectrum depending on the luminescent materials used. The demonstration of spectrally narrow emission in optically pumped thin organic films even in the presence of injecting metallic contacts is an important step towards the possibility of producing electrically pumped solid-state lasers from conjugated polymers and small molecules [1].

The additional exciton quenching due to the presence of polarons increase the required performances of the lasing active material to be used in an electrically driven device. Lowering ASE threshold diminishes the current density required to achieve electrically-pumped lasing emission and reduces the polaron-induced absorption in the “gain” medium [2]. So great efforts are devoted to synthesizing new materials and to engineering new device structures with lower ASE

*Corresponding author: s.toffanin@bo.ismn.cnr.it

threshold and enhanced net gain coefficient. In this way it would be possible to achieve lasing emission in real devices at an achievable current density even in the presence of residual exciton quenching and photon losses.

In order to realize efficient organic solid-state lasers one can employ films of highly luminescent conjugated polymers [3] or alternatively utilize diluted dispersion of dyes or conjugated molecules embedded in host matrix that can act either as dispersive medium [4] or as donor in energy transfer processes [5].

Thin-film vacuum deposition of small organic molecules provides the advantage of a better control on the film morphology and the possible implementation in a multilayer device structure. Instead conjugated polymers can be easily processable from solutions to realize simplified single-layer structures.

The use of a binary blend in which Förster energy transfer between an absorptive donor and an emissive acceptor takes place allows reducing the optical losses in the thin-film waveguides and decreasing the ASE threshold.

Apart from the enhanced optical performances of the blend system with respect to the single-material systems, in case of a matrix with good charge transport properties the binary approach allows exploiting charge transport for the realization of opto-electronic organic devices such as organic light-emitting diodes and transistors and eventually electrically-pumped organic lasers. Moreover the matrix doping with small energy-gap molecules facilitates the implementation of energy-transfer blends as charge-recombination and light-emission layers in multilayer-based opto-electronic devices.

Hereafter we present a new host-guest lasing system whose optical properties are modulated by an efficient non-radiative Förster energy transfer. The system is obtained by co-evaporation of a oligodiarylfuorene derivative named T3 as host material and the well-known red fluorescent dye 4-(dicyanomethylene)-2-methyl-6-(p-dimethylaminostyryl)-4H-pyran dye (DCM) as guest material (see Figure 1 for molecular structures). T3 presents intriguing characteristics, such as high glass transition temperature, high thin-film PL quantum yield in pure blue [6], ambipolar electrical characteristics in time of flight (TOF) measurements [7] and field-effect charge transport [8]. Moreover T3 ASE threshold and net gain are very competitive with respect to the most efficient polymeric and host-guest systems [9].

We investigate how the guest concentration modifies the energy transfer dynamics and ASE properties of the host-guest system [10]. A spectroscopic study is performed to determine the guest concentration at which the ASE threshold is the lowest.

We implement the DCM:T3 blend at a suitable doping concentration in an OLED structure in order to verify the feasibility of the host-guest system in light-emitting devices.

2. EXPERIMENTAL METHODS

For the spectroscopic study DCM:T3 thin-films of 150 nm nominal thickness were prepared by thermal evaporation under high vacuum at a base pressure of 5×10^{-7} mbar onto quartz substrates. The deposition rate was kept constant at $0.3 \text{ \AA} \times \text{s}^{-1}$ for each material. The different volume ratios of T3 and DCM were obtained by reducing the flux of one of the components on the substrate with a mechanical chopper placed in front of the sublimation source. The thin-films of DCM dispersed in a PMMA matrix were obtained by spin-coating an ethyl lactate solution of PMMA with 1% in weight of DCM.

The OLED substrate, consisting in 150 nm-thick film of Indium-Tin Oxide (ITO) deposited on glass, was cleaned according to well-established wet procedure (multiple sonications of dichloromethane, acetone, ethanol and UHP water) in order to remove possible organic contamination.

T3 and DHF4T thin-films in the OLED structure were grown at a fixed rate of 0.3 and $0.1 \text{ \AA} \times \text{s}^{-1}$ respectively by thermal evaporation under high vacuum at a base pressure of 5×10^{-7} mbar. The Au electrodes were deposited in high vacuum at a base pressure of 2×10^{-4} mbar at a growth rate of 0.5 \AA/s . All the thermal deposition are carried out keeping the substrate at room temperature.

UV-visible absorption spectra were recorded with a JASCO V-550 spectrophotometer, while PL spectra were collected in transmission by a Hamamatsu multichannel optical analyzer exciting the samples with the 325 nm and 440 nm lines of a Kimmon He-Cd cw laser. A GG475 cut-off filter is used for cutting the 440 nm excitation without modulating the PL emission.

PL quantum yield measurements were carried out in a Labsphere integrating sphere using as excitation sources either a Oxixus 375 nm laser diode or a 440 nm Kimmon cw He-Cd laser and a calibrated Hamamatsu multichannel optical analyzer as a detection system. All the measurements were performed in air.

The ASE properties of thin-films were measured exciting with the third harmonic of a Q-switched Quantel Nd:YAG laser delivering 25 ns-long pulses at 355 nm with a 10 Hz repetition rate. The laser intensity was adjusted before

impinging on the sample by using neutral density filters and the pumping energy was monitored using a calibrated laser energy meter (Scientech). An adjustable slit and a cylindrical lens were used to shape the laser beam into a strip with a width of 1 mm and a length of 4 mm. The films were pumped at normal incidence with the long axis of the pump beam perpendicular to the edge of the sample. The output signal was focus on a fiber-coupled Hamamatsu multichannel optical analyzer by a lens system. Measurements were performed in vacuum at 20 K.

3. RESULTS AND DISCUSSION

3.1 Steady-state spectroscopic properties

In the system we are considering the T3 thin-film matrix acts both as the donor and the host while the dispersed DCM molecules are the acceptors.

As it can be seen from Figure 1, there is a large overlap between emission spectrum of T3 thin-film and absorption spectrum of the DCM dilute solution which is a necessary prerequisite to achieve efficient Förster resonance energy transfer in the host-guest system.

According to this theory [11] the rate of energy transfer from excited donor (D) to unexcited acceptor (A) is given by

$$K_{DA} = \frac{1}{\tau_D} (R_0/R_{DA})^6 \quad (1)$$

where τ_D is the lifetime of donor in absence of acceptor, R_{DA} is the distance between the donor and the acceptor molecules and R_0 is the Förster radius defined as the distance between donor and acceptor at which energy transfer to the acceptor or decay on the donor occurs with equal probability. R_0 is expressed as

$$R_0^6 = \frac{9000(\ln 10) \langle k^2 \rangle \Phi_D}{128\pi^5 n^4 N_A} J \quad (2)$$

where Φ_D is the donor quantum yield in absence of excitation energy transfer, n is the refractive index of the medium, N_A is the Avogadro's number and k^2 is the molecular orientation factor (for a fixed donor and a random distribution of fixed acceptors $\langle k^2 \rangle = 0.476$ [12]). J is the overlap integral between the donor fluorescence and the acceptor absorption expressed in frequency scale which depends on the acceptor molar decadic extinction coefficient and on the donor fluorescent intensity.

From the overlap spectra of 10^{-5} M toluene solution of DCM molecules and a neat T3 thin-film we calculated an integral overlap of about $1.2 \times 10^{-13} \text{ M}^{-1} \text{ cm}^2$. Considering the T3 refractive index $n=1.75$ [6] and the measured T3 thin-film quantum yield of 47%, the estimation of the Förster radius is 36 Å.

In Figure 2a we report the absorption spectra of DCM:T3 blends obtained by increasing DCM concentration during the sublimation in vacuum. The neat T3 thin-film and DCM dilute solution show absorption spectra peaked at ~383 and 463 nm respectively. The blends spectra (which are normalized to T3 peak in Figure 2a) are simply the linear combinations of the absorption of the pristine materials in the specific molar concentration, except for the slightly blue-shift in the DCM peak probably due to intermolecular interaction in the blend. T3 shows high absorbance at each dopant concentration, while DCM absorbance in the blend increases as expected with its concentration.

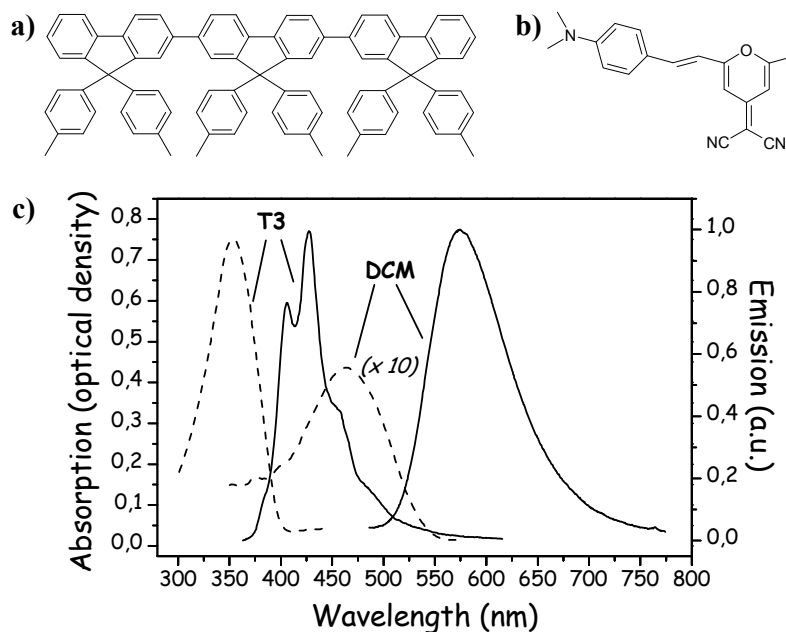


Figure 1. Chemical structure of (a) ter(9,9-diarylfuorene) (T3) and (b) 4-(dicyanomethylene)-2-methyl-6-(p-dimethylaminostyryl)-4H-pyran (DCM). c) Absorption spectra (dashed line) and photoluminescence spectra (solid line) of a 10^{-3} M solution of DCM molecules dissolved in dichloromethane and of a 100 nm-thick T3 film grown by thermal evaporation.

In Figure 2b the normalized photoluminescence (PL) spectra of the DCM:T3 blends at different concentrations are reported. The direct DCM emission is almost negligible at the excitation wavelength used (325 nm). T3-alone PL shows a vibronically resolved spectrum typical of polyfluorenes with the highest oscillator strength in correspondence of the 0-1 transition at 428 nm [13], while the emission from DCM molecules dispersed in a PMMA matrix is broad, since the full-width at the half maximum (FWHM) value is around 91 nm, featureless and peaked around 562 nm. In the spectra of the composite films there is the clear evidence of energy transfer from T3 to DCM, since increasing DCM concentration the T3 component gradually disappears (in 10% and 20% samples is completely absent).

As the guest concentration is increased the DCM peak monotonically red-shifts from 570 nm for the 2% sample to 607 nm for the 20% sample and the FWHM values increase from 98 nm for the 2% sample to 108 nm for the 20% sample. We can infer that DCM molecules dispersed in a solid matrix of T3 undergo an energy shift due to self-polarization for the more dilute samples and to real aggregate formation for the more concentrated ones. As the concentration of highly polar DCM molecules (dipole moment at ground state $\mu_g = 6.1$ D [14]) in relatively non-polar T3 is increased, the distance between nearest-neighbour DCM molecules decreases, thereby increasing local electrical field experienced by DCM molecules. In general, polar dopants, such as DCM, tend to arrange locally in oriented domains that minimize the overall energy of the system, causing a spectral red shift with respect to the isolated molecules [15].

For better understanding the role of the matrix on DCM emission features, we performed PL measurements exciting only the guest molecules in the blends. As it can be seen from Figure 3, the DCM peak wavelengths and FWHM are almost the same regardless the fact that the DCM PL emission is collected either after excitation transfer from the host molecules or following direct excitation of the guest molecules. It seems that after the excitation is transferred, T3 matrix acts just as a host material without altering the emission properties of the acceptor molecules. So it is likely that using this blend as a recombination layer in a device the electroluminescent emission would remain the same regardless the processes that brings DCM molecules in the electronic excited state, i.e. exciton transfer from the donor molecules or direct charge trapping in acceptor molecules.

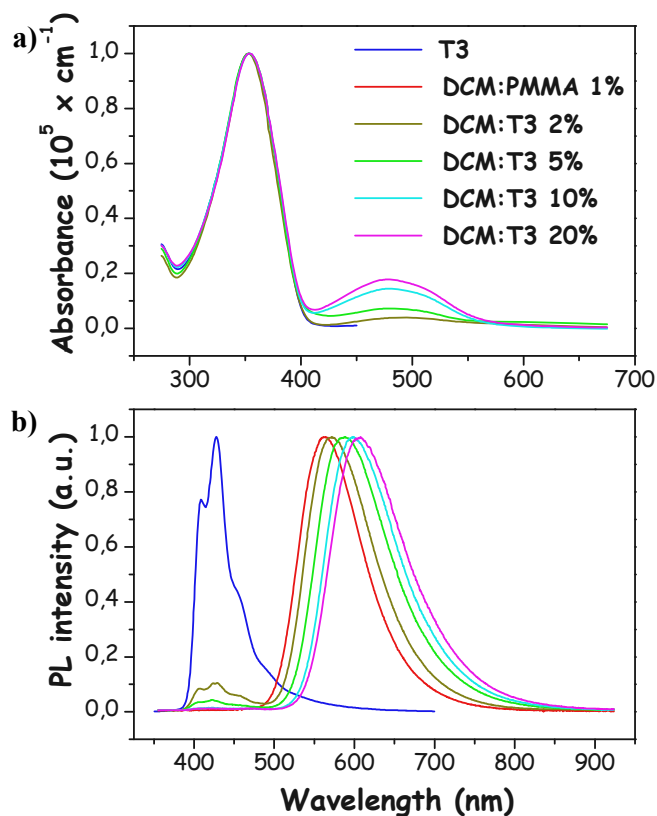


Figure 2. a) Absorption spectra of thin films of different DCM:T3 blends with increasing DCM molar concentration and of T3 alone. All the spectra are normalized with respect to T3 alone absorption peak. b) Photoluminescence spectra of thin films of different DCM:T3 blends with increasing DCM molar concentration obtained by exciting the donor component. The spectra of neat T3 thin-film and of the solid solution of DCM dispersed in PMMA at 1% in weight are reported. Photoluminescence spectra are normalized with respect their own maxima.

Also PLQY measurements seem to indicate the interaction among DCM molecules even at relatively low concentration. As it can be seen in Table 1, although the PLQY of the DCM molecules dispersed in PMMA matrix is around 70% the quantum efficiency of the blend system is not improved with respect to that of the pure T3 host. The 2% sample shows the highest PLQY while in the 10% and 20% samples it is severely quenched as expected when physical aggregates are formed. PLQY measurements exciting exclusively and directly the DCM molecules (440 nm excitation wavelength) show a similar trend. However in the latter case the absolute PLQY are higher. This points to the fact that the energy transfer process affects the overall quantum yields of the blends.

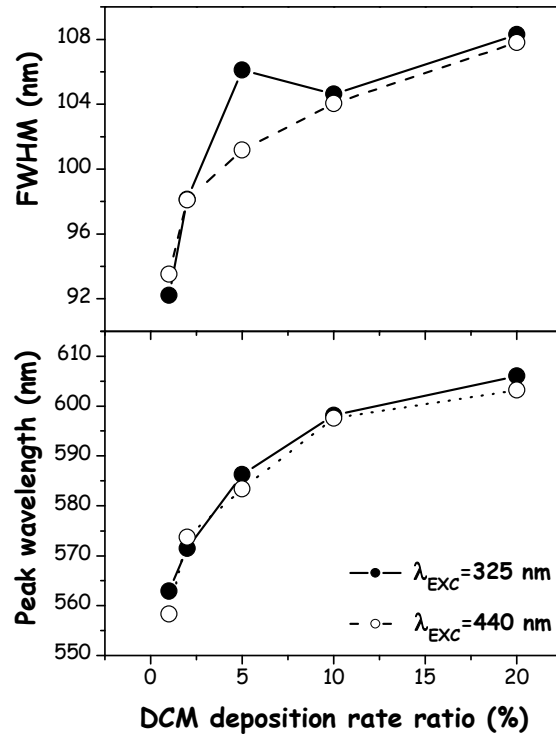


Figure 3. Full width at half maximum (FWHM) values and peak wavelengths of DCM photoluminescence maxima with increasing DCM concentration. Donor and the acceptor molecules are selectively excited at 325 nm and 440 nm.

	T3	2%	5 %	10 %	20 %	DCM
PLQY @ 375 nm	0.46	0.25	0.12	0.07	0.06	0.7
PLQY @ 440 nm	-	0.4	0.21	0.1	0.08	0.6
ASE THRESHOLD (kW/cm ²)	4.4	0.6	1.1	2.8	3.8	-

Table 1. Photoluminescence quantum yields (PLQY) of DCM:T3 blends with different DCM concentrations together with the values obtained from neat T3 thin-film and a solid solution of DCM dispersed in PMMA at 1% in weight. We selectively excite the donor or the acceptor components of the blends by using the 375 nm and the 440 nm wavelengths respectively.

We report also the values of the amplified spontaneous emission (ASE) thresholds for the blends and T3-alone thin-films

3.2 ASE threshold

In Table 1 we report the ASE pump intensity thresholds with varying DCM concentrations in the blends together with the T3-alone value. The ASE threshold is defined as the pump intensity at which the FWHM is reduced to half the FWHM of the PL at low pump intensity.

The ASE peaks located always in the DCM emission region regardless the dopant concentration reveal that upon T3 molecules excitation the energy transfer towards DCM molecules dominates over the T3 stimulated emission process. Considering the laser exciting pulse (25 ns at FWHM) as steady-state compared with the energy transfer and radiative decay timescale in the system, we can assign the energy transfer rate in the first 20 ps in the 2% sample as an inferior limit for the ASE rate value in the neat T3 thin-film.

Increasing DCM concentration the energy transfer rate seems to increase while ASE threshold does not reduce. It is worthy noting that in ASE spectrum of the 20% sample the DCM ASE peak is much broader and the T3 emission component is clearly visible (but completely absent in the steady-state transmission spectrum) as if T3 and DCM ASE processes were competing (Figure 7). Moreover the lowest ASE threshold value is found in correspondence of the 2% sample, indicating that the spontaneous emission guided through the exciting stripe is very sensitive to the aggregation state of the emitting molecules.

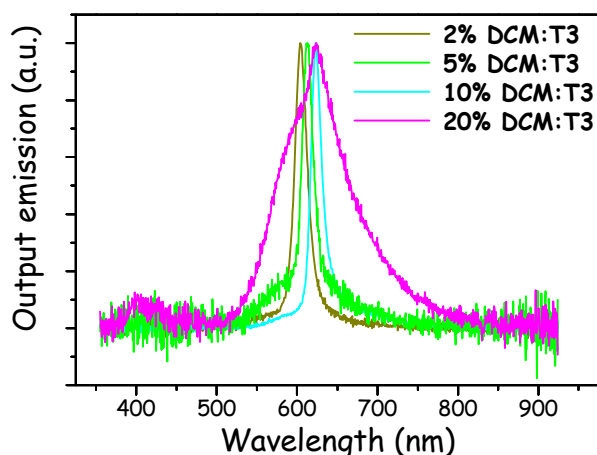


Figure 4. Normalized DCM:T3 blends emission spectra collected from the edge of a 4 mm²-wide excitation stripe. The pump intensity is higher than the ASE threshold.

It can be seen that the ASE peak is located in the low energy side of the PL spectrum because the higher net gain always takes place at the peak far from the absorption edge that would introduce self-absorption [16]. We also note that the ASE peak shift with respect PL peak decreases with increasing DCM concentration. Since the films present nominally the same thickness (about 150 nm), it is likely that the ASE wavelength position for higher concentration samples could be induced by excited-states absorption (reducing net gain at larger wavelengths) rather than amplification of different modes due to cavity effects. Consistently photoinduced absorption measurements on ms timescale carried out on T3 alone thin-film show a broad peak centred at 690 nm that is assigned to triplet–triplet absorption from the lowest T₁ to a generic upper lying T_n state [17].

3.3 Electroluminescence characteristics

In order to verify the optical properties of the new host-guest system in real working light-emitting devices we optimized, the DCM:T3 blend is inserted as recombination layer in an OLED structure. In the devices we fabricated (Figure 5) we implemented as hole transport layer a 30 nm-thick T3 thin-film since it is well known from time of flight measurements that this amorphous material shows non-dispersive vertical charge transport [7].

To realise the central light-formation layer 10 nm-thick DCM:T3 blend with 5% weight doping concentration is grown on top of T3 layer. From the spectroscopic study it was established that the 5% doping concentration can guarantee efficient energy transfer (though not complete) between donor matrix and the acceptor molecules without degrading drastically the optical properties of the blend because of the donor aggregation. Since the residual T3 emission of in the PL spectrum of the 5% blend, we expect to fabricate a white light-emitting OLED.

Finally a 60 nm-thick thin-film of a fluorinated derivative of quarter-thiophene (α,ω -diperfluorohexyl-quaterthiophene) named DHF4T [18] is implemented as electron-transport layer. DHF4T is extensively used as electron-transport layer in organic field-effect transistors since in DHF4T thin-films molecules arrange in crystalline domains in a way that field-effect transistor devices show high planar charge mobility values [19]. Anyhow, the typical 3D growth DHF4T thin-films with the formation of thick elongated pillars assures also vertical electron transport in nanometric length scale.

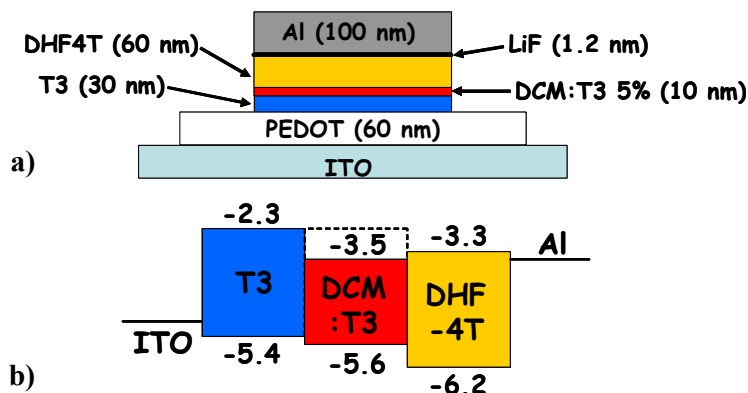


Figure 5. a) Schematic representation of the OLED device implementing the DCM:T3 blend as recombination layer with indication of the thickness of each layer. b) Energy level diagram of the tri-layer heterostructure. The energy values of the HOMO and LUMO levels of each molecular material are indicated together with the Fermi level of the gold contacts.

Considering the energy level diagram of the T3/T3:DCM/DHF4T organic heterostructure reported in Figure 5b, ITO and Al/LiF electrodes are used because they can guarantee efficient hole and electron injection respectively. It is likely that excitons can be formed on T3 matrix in the recombination layer and then transferred to DCM molecules where the light formation takes place, if electrons are able to overcome the 1 eV energy barrier at the interface between T3 and DHF4T thin-films.

Nevertheless we cannot exclude *a priori* that excitons could be formed by other mechanisms. Given the thickness of the recombination layer and the overall energetic of the system it can also be plausible that electrons are directly transferred to DCM molecules, which in turn act as a charge traps for the holes percolating in T3 matrix. In any case when both the charges are in DCM molecules they cannot easily migrate or be transferred to other molecular sites due to the unfavorable energetic barriers they should overcome.

As it can be seen in Figure 6, the opto-electronic characteristics of the OLED device follow a typical OLED behavior. The current increases exponentially by increasing the applied anode-cathode voltage with the light emission intensity following the same trend. Evidently the applied bias voltage is sufficiently low to avoid noticeably the charge-exciton process which is responsible of the characteristic OLED electroluminescence intensity plateau above a critical value of the injection current.

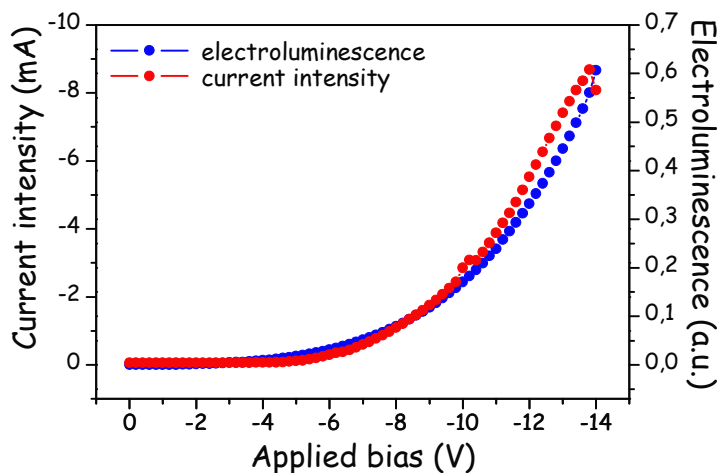


Figure 6. Opto-electronic characteristics of the OLED sketched in Figure 5a.

The OLED electroluminescence (EL) spectrum (Figure 7) extends on almost the entire visible wavelength range displaying two maxima in the correspondence of the T3 and DCM emission regions. Indeed, the emitted light is white.

So the light-formation process only partly takes place on DCM molecules in the recombination layer since the EL in the blue range is too intense to be due to the residual emission of T3 molecules in the blend. Given the very high PLQY of T3 thin-films, it is likely that excitons form and annihilate radiatively also in the hole transport layer once electrons happen to populate T3 LUMO. Moreover we cannot exclude that also the DHF4T can participate in the electroluminescence process even if this material in thin-film is poorly emissive.

The optimization of the thickness of the different layers in the heterostructure together with the insertion of an electron-blocking layer at the T3/DCM:T3 interface should be necessary for fabricating a device in which the light formation takes place only in the recombination layer.

Anyhow, the red emission from DCM molecules is much more intense than the other spurious signals and located at the same wavelength of the PL spectrum of DCM molecules in the 5% blend, as we expected.

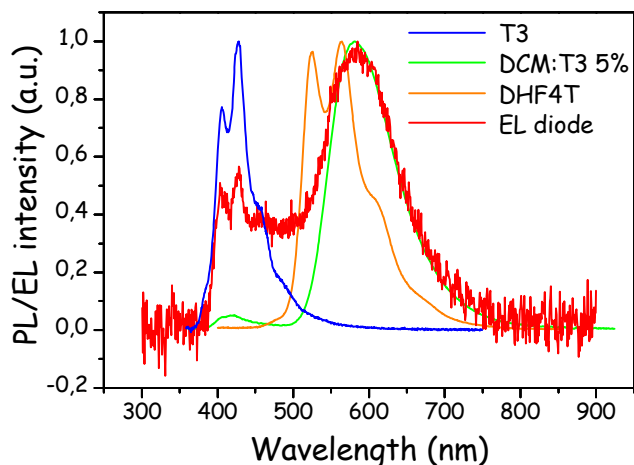


Figure 7 Electroluminescence spectrum of the OLED compared with the photoluminescence spectra of the single layers composing the overall heterostructure.

It is interesting to note that the heterostructure presented can be easily implemented as active region in light-emitting organic field-effect transistors (OLETs) since both the hole [19] and electron transport [8] materials showed interesting field-effect transport properties in single-layer devices. Indeed, it is well-known that light-formation process is much more efficient in OLETs than in OLEDs [20].

4. CONCLUSION

In conclusion, we investigated the photo-physical properties of the new lasing DCM:T3 system in which an efficient Förster energy transfer takes place from the ambipolar semiconducting matrix T3 to the lasing molecule DCM. By varying the guest concentration, we studied the energy transfer dynamics finding out that the non-radiative energy transfer is Förster-like only for the lowest guest concentration sample. For higher guest concentrations the energy transfer becomes much faster but the overall dynamics is ruled by the guest interaction and aggregation.

The mirrorless lasing measurements performed on the blends reveal that the lowest ASE threshold is presented by the blend in which the guest aggregation is almost negligible and the energy transfer is incomplete.

To investigate electroluminescent activities of this new host-guest system we fabricated test OLED devices inserting the DCM:T3 blend as recombination layer between T3 and DH4T thin-films that worked as hole and electron transport layers respectively. The 5% doping concentration in the matrix was chosen to guarantee an efficient energy-transfer process and low dipolar interaction among DCM molecules. The EL emission is white with the dominating red component originating from the emission of the doping molecules in the blend. Further spectroscopic investigation on the

working devices are necessary for comprehending which specific process (charge trapping, energy transfer,...) in the host-guest blend is responsible for the light emission.

The very low ASE threshold together with the ambipolar charge-transport characteristics of the T3 matrix, makes DCM:T3 a very attractive candidate to be used as a gain medium for the fabrication of organic solid-state lasers. Indeed, reducing the ASE threshold to ultra-low values is one of the key parameters that allows reducing the required current density and the polaron-exciton interaction in the gain medium of an electrically-pumped devices.

ACKNOWLEDGEMENTS

This work was supported at Bologna by EU under projects FP6-IST-015034 (OLAS) and EU-FP6-Marie Curie-035859 (BIMORE) and by Italian Ministry MIUR under Projects FIRB-RBNE033KMA, FIRB-RBIP06JWBH (NODIS) and FIRB-RBIP0642YL (LUCI). Authors thank M. C. Ramon for the help in the ASE threshold measurements of DCM:Alq₃ sample and R. Zamboni for stimulating discussions.

REFERENCES

- [1] Yokoyama, D.; Nakanotani, H.; Setoguchi, Y.; Moriwake, M.; Ohnishi, D.; Yahiro, M.; Adachi, C. *Jpn. J. Appl. Phys.* **2007**, *46*, L826-L829
- [2] Yamamoto, H.; Kasajima, H.; Yokoyama, W.; Sasabe, H.; Adachi, C. *Appl. Phys. Lett.* **2005**, *86*, 83502-83503.
- [3] Xia, R.; Heliotis, G.; Bradley, D. D. C. *Appl. Phys. Lett.* **2003**, *82*, 3599-3601.
- [4] Nakanotani, H.; Akiyama, S.; Ohnishi, D.; Moriwake, M.; Yahiro, M.; Yoshihara, T.; Tobita, S.; Adachi, C. *Adv. Func. Mater.* **2007**, *17*, 2328-2335.
- [5] Zhang, D.; Ma, D. *Appl. Phys. B* **2008**, *91*, 525-528.
- [6] Lin, H. W.; Lin, C. L.; Chang, H. H.; Lin, Y. T.; Wu, C. C.; Chen, Y. M.; Chen, R. T.; Chien, Y. Y.; Wong, K. T. *J. Appl. Phys.* **2004**, *95*, 881-886.
- [7] Wu, C. C.; Liu, T. L.; Hung, W. Y.; Lin, Y. T.; Wong, K. T.; Chen, R. T.; Chen, Y. M.; Chien, Y. Y. *J. Am. Chem. Soc.* **2003**, *125*, 3710-3711.
- [8] Oyamada, T.; Chang, C. H.; Chao, T. C.; Fang, F. C.; Wu, C. C.; Wong, K. T.; Sasabe, H.; Adachi, C. *J. Chem. Phys. C* **2007**, *111*, 108-115.
- [9] Lin, H. W.; Lin, C. L.; Wu, C. C.; Chao, T. C.; Wong, K. T. *Org. El.* **2007**, *8*, 189-197.
- [10] Camposeo, A.; Mele, E.; Persano, L.; Pisignano, D.; R. Cingolani, R. *Phys. Rev. B* **2006**, *73*, 1652011-1652017.
- [11] T. Förster, et al., *Modern Quantum Chemistry, Part 2 : Action of Light and Organic Molecules* (Academic, New York, 1982).
- [12] Rozman, I. M. *Opt. Spectrosc.* **1958**, *4*, 536-538.
- [13] Salbeck, J.; Yu, N.; Bauer, J.; Weissörtel, F.; Bestgen, H. *Synth. Met.* **1997**, *91*, 209-215.
- [14] Kwak, G.; Okada, C.; Fujiki, M.; Takeda, H.; Nishida, T.; Shiosaki, T. *Jpn. J. Appl. Phys.* **2008**, *3*, 1753-1756.
- [15] R. Farchioni, G. Grosso, *Organic Electronic Materials* (Sprinter-Verlag Berlin Heidelberg 2001).
- [16] McGehee, M. D.; Heeger, A. J. *Adv. Mater.* **2000**, *12*, 1655-1668.
- [17] Cabanillas-Gonzales, J.; Sciascia, C.; Lanzani, G.; Toffanin, S.; Capelli, R.; Ramon, M. C.; Muccini, M.; Gierschner, J.; Hwu, T. Y.; Wong, K. T. *J. Phys. Chem B* **2008**, *112*, 11605-11609.
- [18] Facchetti, A.; Deng, Y.; Wang, A.; Koide, Y.; Sirringhaus, H.; Marks, T. J., Friend, R. H. *Angew. Chem. Int. Ed.* **2000**, *39*, 4547-4551.
- [19] Facchetti, A.; Mushrush, M.; Katz, H. E.; Marks, T. J. *Adv. Mater.* **2003**, *15*, 33-38.
- [20] Muccini, M. *Nature Mat.* **2006**, *5*, 605-613.